

42 However, most of the available simulation systems either rely on rather simple
43 pedestrian navigation models, which reflect real human behavior only in a very limited
44 manner, or are computationally expensive. This paper contributes to enhancing
45 computationally cheap pedestrian simulation models by presenting a sophisticated graph-
46 based approach for modelling navigational behaviour of humans. This allows engineers and
47 architects to quickly and effortlessly evaluate different layout options. The implementation of
48 this approach includes an advanced technique for generating sparse navigation graphs from a
49 given spatial layout of the scenario under investigation.

50 **2 Related work**

51 The simulation of pedestrian crowds has been widely examined using a variety of approaches
52 that focus on different details depending on the objective of the simulation [1]. For example,
53 to determine minimum evacuation times for buildings or areas, macroscopic models are
54 typically used. These focus on the overall situations of the simulated scenario and are based
55 on mean values. Examples of such models are network flow models [2], fluid-dynamic
56 models [3] or gas kinetic models [4]. To simulate the individual behaviour of pedestrians on
57 the other hand, microscopic models have been developed. These models consider the
58 movements of each individual and focus on the interaction between individuals. Force models
59 (e.g. Social Force Model by Helbing and Molnár [5]) as well as cellular automata [6] or
60 agent-based models [7] belong to this category.

61 One central aspect of microscopic pedestrian simulation is to simulate the different movement
62 strategies of individuals. Pelechano and Malkawi [8] categorize “virtual human technologies”
63 into different features, such as appearance, function, time, autonomy and individuality.

64 The focus of this contribution lies on the latter: to differ between individual behaviour as a
65 factor of sex and age, and – the authors’ main focus – sense of orientation and familiarity with
66 a location. The aim is to simulate large pedestrian crowds while taking into account different
67 movement behaviours. An important constraint considered for the development of the
68 corresponding algorithms is the requirement of high computational performance which allows
69 for real-time simulations even on standard hardware. This provides the possibility to use the
70 simulator as training facility for preparing and training the security staff of major events. – a
71 feature strongly demanded by security authorities.

72 In order to assign individual behaviour to pedestrians, agent-based models are common.
73 These assign different behavioural patterns to each individual, which results in different
74 movement behaviour. Reynolds [9] models the perception of individuals with three different
75 layers, namely a locomotion layer, a steering layer and an action selection layer. Musse and
76 Thalmann [10] developed a human crowd behaviour model, consisting of a random
77 behavioural model, which can be described by a few parameters. In [11], a personality model
78 is mapped into a simulation model. Taking this a step further, Lerner [12] uses tracking from
79 video data to obtain possible movements and trajectories. As these models have to calculate
80 the new position of each pedestrian according to a complex set of rules in every time step,
81 they are very computationally intensive and are capable of simulating only few pedestrians in
82 real time. Another, faster way to assign individual behaviour is to use a navigation graph with
83 different routing algorithms according to the individuals’ preference. Since the objective is to
84 simulate a large crowd in a large area in real time, the latter approach has been chosen.

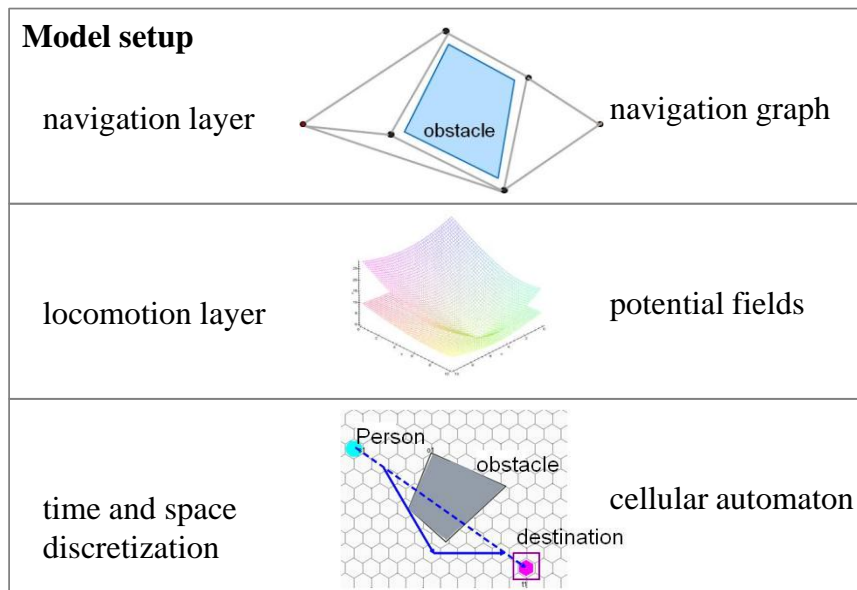
85 Combining a microscopic layer with such graphs or networks was proposed by [13]. Here, a
86 continuous microscopic model is used as operational model, i.e. to model the microscopic
87 pedestrians’ movement, in combination with a tactical model implemented as a network, for
88 pedestrians’ route assignment. The network consists of uniform square cells, which are

89 connected by links. [14] combines an agent-based approach with a macroscopic network. In
90 spite of taking cost functions and optimizing the flow, agents move through this network
91 choosing the next vertex based on different criteria. The authors call this algorithm route
92 choice self organisation (RCSO). However, both approaches do not focus on the derivation of
93 a graph from a given geometry but take either such a network as given or simply divide space
94 into uniform squares, the latter resulting in unrealistic wayfinding behaviour.
95 In contrast, this paper describes a technique for generating navigation graphs based on
96 navigation points, which precisely reflect human navigational behaviour. At the same time,
97 the graph consists of a minimum number of edges and vertices, enabling a high computational
98 efficiency of the corresponding navigation algorithms.
99 A variety of alternative techniques have been proposed to create a navigation graph or
100 roadmap from a given topography. Most of these techniques have been developed in the field
101 of Robotics. [15] gives a good overview of the most common techniques of space
102 decomposition. [16] describes all kind of planning algorithms, including motion planning
103 algorithms. One technique for deriving a roadmap is to divide the space with Generalized
104 Voronoi Diagrams [17] and to use the resulting lines as graph edges and the intersection
105 points of the lines as graph nodes. The resulting graph consists of edges which are equidistant
106 to each obstacle. A similar approach has been proposed in [18]: Here, agents navigate along
107 combined Voronoi diagrams, which include not only obstacles but other moving agents as
108 well. The intersection of the regions of the first order Voronoi diagram with the second order
109 Voronoi diagram forms the navigation graph. The authors call this graph Multi-agent
110 Navigation Graph (MaNG), which provides maximal clearance for each agent. This kind of
111 graphs is suitable for steering robots, however they do not reflect human navigational
112 cognition and are therefore of only limited applicability for pedestrian simulation.
113 Approaches which are capable to more accurately model human perception and cognition are
114 based on visibility graphs [15]. A visibility graph consists of vertices defined by sources,
115 destinations and obstacles within a scenario. Two nodes are connected if they are in line-of-
116 sight. To avoid redundant edges, a reduced visibility graph can be constructed by categorizing
117 edges into supporting and separating edges [15]. In [19], such a visibility graph is used to
118 navigate agents through a scenario. Based on this visibility graph, a pre-computed shortest
119 path map is stored. If other moving agents are located on the pre-calculated path, a
120 recalculation has to be performed. Since this recalculation is very computational intensive, the
121 focus of Choset's work lies on the approximation of agents' positions in order to minimize the
122 number of recalculations by excluding agents which are outside the viewable region of the
123 subject under examination. Gloor et al. [20] propose to construct a visibility graph by placing
124 nodes at a certain distance from convex corners. This approach prevents simulated pedestrians
125 from walking too close around a corner, but it also produces many nodes, which are
126 dispensable.
127 In this paper we describe a novel navigation graph generation algorithm which is based on the
128 idea of placing nodes at a certain distance from each corner, but discards all superfluous
129 nodes. Furthermore, the resulting graph is not as dense as a common visibility graph because
130 geometrically close edges are omitted.

131 **3 Model setup**

132 An important requirement is that the simulator is able to run in real time, as the simulator is
133 designed as a training tool. To achieve such high performance, a cellular automaton model for
134 space discretization in combination with a conservative force model [21] has been chosen, i.e.
135 a model based on energy potentials that describe the influencing forces on each pedestrian

136 (attracting force of the destination, repellent forces of obstacles as well as the repellent forces
 137 of other pedestrians). Combining the cellular automaton with these forces, the navigation of
 138 single pedestrians can be modelled efficiently [22]. This combination makes it possible to
 139 quickly update pedestrians' positions while taking into account the interactions between them.
 140 However, using this approach key aspects of pedestrian movement are neglected, namely the
 141 individual navigational behaviour of pedestrians as well as the large-scale orientation of
 142 pedestrians. Using only the cellular automaton model, the simulated pedestrians appear as
 143 being short-sighted, since only neighbouring cells are considered in each update step.
 144 In order to take into account different degrees of knowledge of efficient routes towards a
 145 destination as well as individual navigational behaviour (e.g. keep as close as possible to the
 146 direction to the destination, choose routes with less turns, etc.) without losing computational
 147 speed, the basic model is extended in our proposal by a navigation graph. Pedestrians move
 148 according to the cellular automaton from one graph node to the next. The graph models the
 149 large-scale orientation of pedestrians. Thus the pedestrians' decisions can now also be
 150 influenced by events at the edges. An overview of the hierarchical setting of the model is
 151 illustrated in Figure 1. Using this graph approach, different route choice behaviours can be
 152 implemented and thus different pedestrian types (e.g. pedestrians who are / are not familiar
 153 with a particular environment).
 154 The navigation graph is based on the concept of visibility graphs. However, our method
 155 differs from the method described in [15] and [20]. First, navigation points are constructed
 156 that will serve as graph vertices and then these vertices are connected according to criteria
 157 depending on the location of the sources and destinations of a scenario.
 158



159

160

Figure 1 Hierarchical setup of simulation model

161 4 Construction of a navigation graph from a geometric scenario setup

162 During the simulation, pedestrians are routed from vertex to vertex on the navigation graph,
 163 until they reach their destination. Thus, one requirement for a navigation graph is that the
 164 graph represents real routes of pedestrians as closely as possible. The Generalized Voronoi
 165 Diagram (GVD) forms a graph with equidistant edges from each obstacle. By taking a GVD
 166 as a navigation graph, pedestrians would walk equidistant to all obstacles. This would result

167 in large detours. With visibility graphs, the resulting routes are close to obstacle corners and
168 thus reflect human behaviour more realistically. Hence, we rely on visibility graphs as
169 navigation graphs.

170 The derivation of the visibility graph from a given geometry is achieved in multiple steps,
171 which are described in detail below.

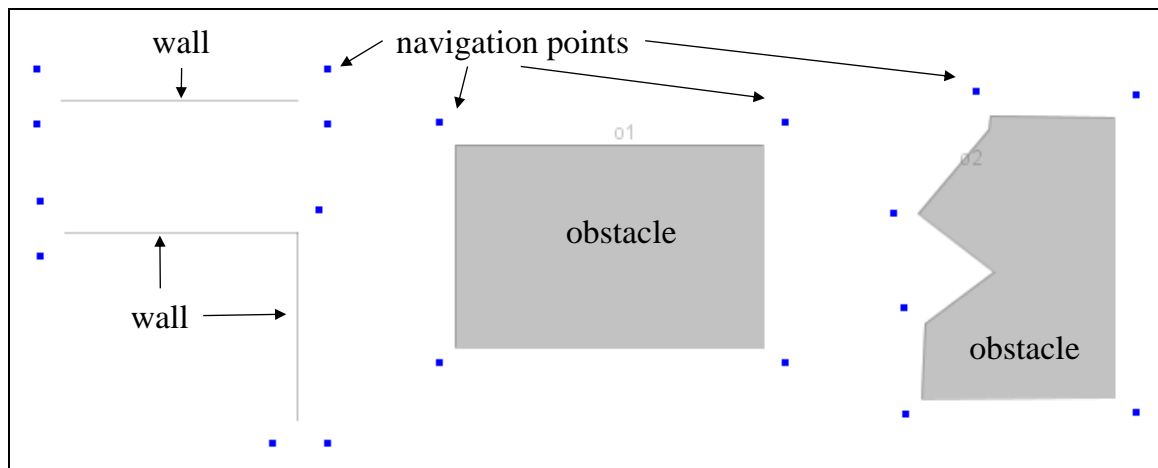
172

173 4.1 Derivation of navigation points (vertices)

174 In the first step, the geometry of a given simulation scenario is examined and navigation
175 points are placed around each obstacle at each convex corner. Each of these points will
176 correspond to a vertex in the visibility graph.

177 Since there are two different types of obstacles – one-dimensional (e.g. walls) and two-
178 dimensional obstacles (e.g. houses) – placement of navigation points has to distinguish
179 between these two cases, as illustrated in Figure 2.

180



181

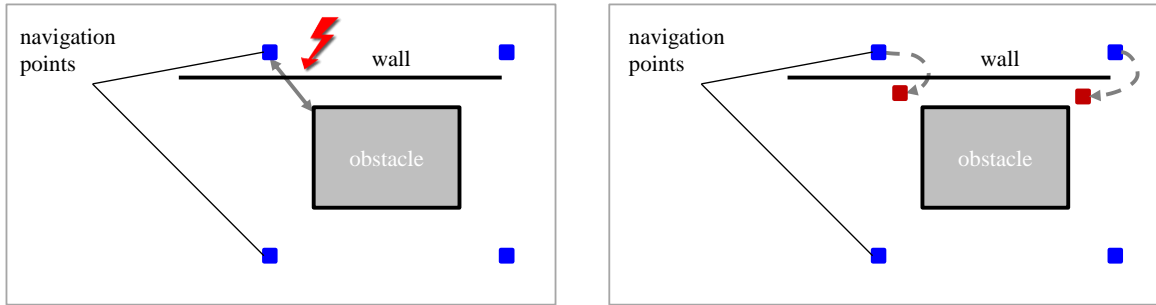
182 **Figure 2 Navigation point placement for walls and obstacles**

183 Depending on the obstacles' geometry, an overlap of two neighbouring navigation points may
184 occur or a corner point is not visible from the corresponding corner. As a result different
185 consistency checks on navigation points are carried out:

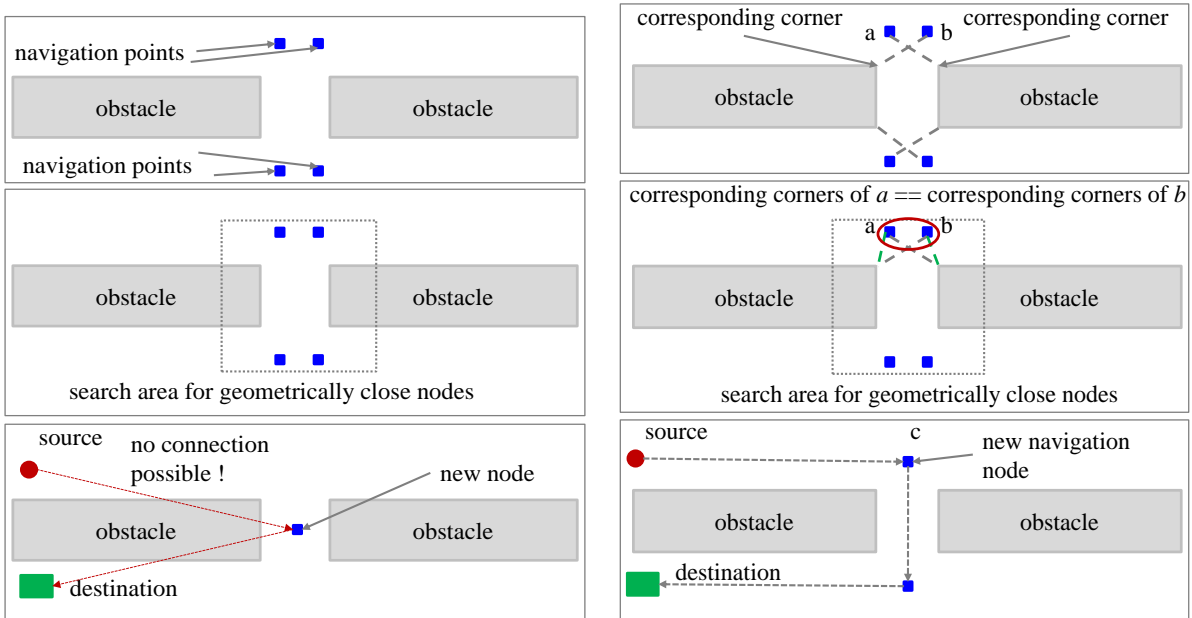
186 • One criterion for a valid navigation point is that the imaginary sight line between the point
187 and the corresponding obstacle corner is not obstructed. If this check fails, the
188 corresponding points are re-located in such a way that they fulfil this criterion. An
189 illustration is given in Figure 3. If the distance between two obstacles is smaller than the
190 length of a cell of the cellular automaton (i.e. no pedestrians is able to walk between the
191 two obstacles), no navigation point is placed. The exact algorithm is described in [23] and
192 [24].

193 • To avoid redundant points, i.e. points which are located geometrically close to one
194 another, a second check is performed. If two or more nodes are located close together, the
195 simplest approach would be to merge them into one single point. But, as can be seen in
196 Figure 4 (left), this may result in non-reachable destinations, since the criterion of
197 visibility between two nodes is not fulfilled (see Section 4.2 Connecting vertices: a cone-
198 based search method for more details). To accommodate this, the following check is
199 implemented: for each navigation point, the corresponding obstacle corner is stored. If
200 another corner point lies closer to the corresponding corner than the navigation point

201 itself, the corresponding corner is added to this point. If the same is true vice versa, then
 202 both points are merged into a new navigation point. This ensures that there is always a way
 203 around each corner. An example of this approach is shown in Figure 4 (right).
 204



205
 206 **Figure 3 Replacement of navigation points so that there are no obstructions between the point and**
 207 **corresponding obstacle corner**
 208

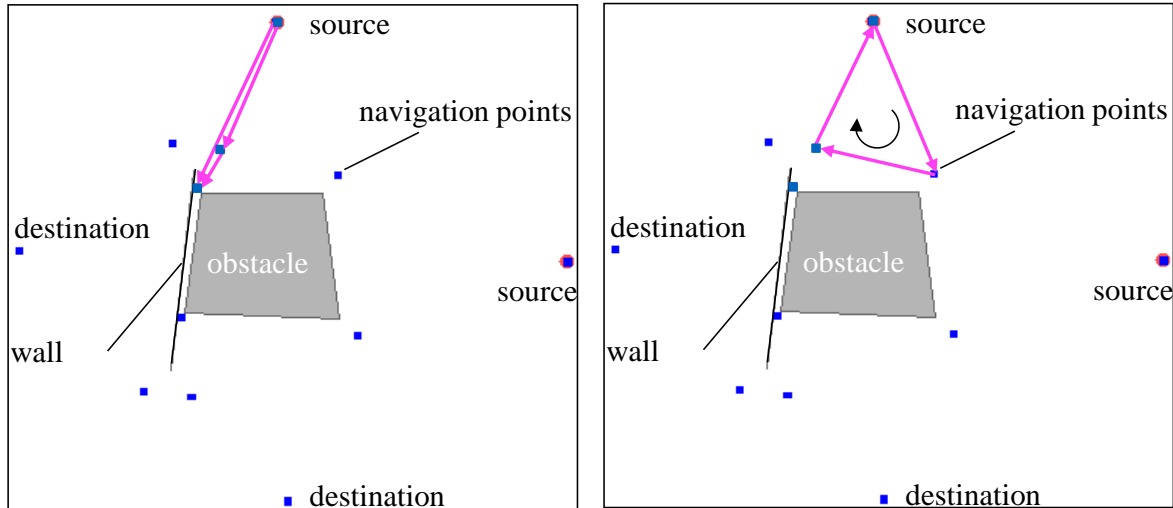


209
 210 **Figure 4 Left: If all geometrically close points are merged, this can lead to non-visibility graphs: as a**
 211 **result, there is no connection around a corner. Right: Correct merging of two adjacent nodes by checking**
 212 **the corresponding corners of each node; only if two nodes have the same corresponding corners are they**
 213 **merged into a new, single point.**

214 **4.2 Connecting vertices: a cone-based search method**

215 Once all navigation points have been created, these points are connected according to certain
 216 rules. The first rule is that two vertices can only be connected if there is a sight line between
 217 them. This is the definition of a visibility graph and a basic requirement for the routing
 218 algorithms, since the Euclidean distance is used to determine edge weights.
 219 The objective is to construct a directed graph, which is able to model human navigation
 220 behaviour in as much detail as possible. However, the inclusion of all possible navigation
 221 options, i.e. all possible edges fulfilling the criterion of visibility, would result in a very dense
 222 navigation graph, which would dramatically decrease computational efficiency. Since the aim

223 is to simulate large crowds in real time, the resulting graph should cover major aspects of
 224 navigation decisions while at the same time being as sparse as possible. To obtain a sparse
 225 graph, redundant edges are avoided. Redundant edges are those that form a loop, i.e. do not
 226 lead to the destination, as well as those that are geometrically located very close to each other.
 227 An example of such edges is shown in Figure 5.
 228



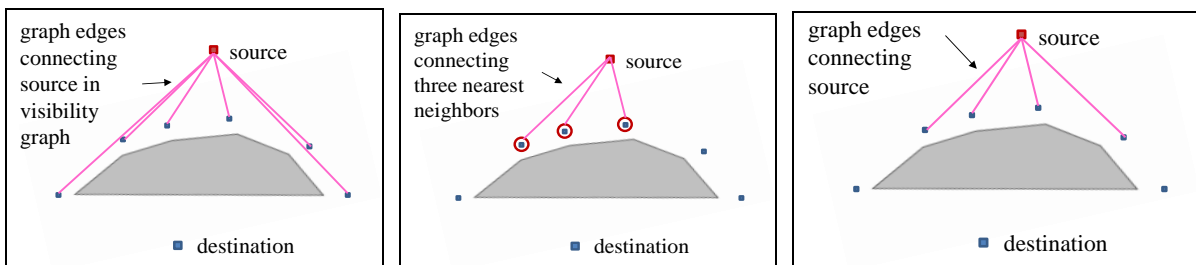
229

230
 231

Figure 5. Redundant edges:
 left, geometrically close edges; right, edges that lead pedestrians back to the source.

232 A spatial index, namely an R*-Tree [25] is used to make visibility graphs more sparse. Using
 233 this data structure, nearest neighbours of a point can be found efficiently in a search space that
 234 exists of one- and two-dimensional objects such as polygons and points. In [24] we propose to
 235 always connect a node with its three nearest neighbour nodes via an edge. However, this
 236 procedure is not sufficiently flexible for arbitrary geometries since cases can occur where
 237 individual vertices have more than three neighbours that need to be connected in order to
 238 cover the full directional range. One example is illustrated in Figure 6: the picture on the left
 239 shows the complete visibility graph, the picture in the centre the resulting edges from the
 240 former method: here, the source is connected with the three vertices inside the red circles, but
 241 the vertices to the far left and far right are not connected. The picture on the right shows the
 242 result of our improved method: the connecting edges lead in every direction. This improved
 243 method is outlined in more detailed below.
 244

244



245

Figure 6: Examples of a geometry, where the algorithm presented in [24] would not find all important neighbouring vertices of a source. Left: a complete visibility graph; middle: connecting the three nearest vertices; right: resulting edges for cone-based method.

249 The algorithm consists of a cone-based search for finding the most relevant neighbours to be
 250 connected. The basic idea is that the angle between two outgoing edges has to be larger than a

251 certain threshold. If the angle is smaller, the longer edge is discarded. The algorithm works as
 252 follows: The graph is initialized by inserting all navigation points as vertices. It starts with an
 253 arbitrary vertex v_i . For this vertex, a rectangular search area is defined, such that the inspected
 254 vertex v_i as well as all destinations of the given scenario are located inside that area.
 255 Furthermore, if any obstacle obstructs the sight lines between v_i and each of the reachable
 256 destinations, the search area is extended until it encompasses these obstacles (
 257 Figure 9a). Inside this area, a search is conducted for all vertices within sight of v_i , sorted
 258 according to their distance to v_i (
 259 Figure 9b). An edge is created between the closest vertex and v_i . Starting from v_i , a cone-
 260 shaped area is defined around the edge with an angle α_{cone} . This cone-shaped area (
 261 Figure 9c) is then subtracted from the search area and the next vertex chosen with the smallest
 262 distance to the vertex v_i . The same procedure is conducted with this vertex, i.e. this vertex is
 263 connected and the corresponding cone-shaped area removed from the search area. The
 264 resulting edges of v_i are shown in
 265 Figure 9d. The algorithm is repeated for every graph vertex. Figure 7 shows the pseudo code
 266 of the algorithm.
 267

Algorithm: Graph construction

Parameters: Set of orientation points; Set of destinations $D \subseteq V$; Obstacles O

Output: Graph $G (V, E)$

1: Add all orientation points as vertices V to G

2: **For** each vertex v_i in $V \setminus D$ **Do**

3: Define search area A_{search} , such that: $v_i \in A_{\text{search}}, \forall d_i \in D \in A_{\text{search}}$

4: **For** all obstacles o_i in line of sight between v_i and $d_i \in D$ **Do**

5: Expand A_{search} , such that all orientation points of $o_i \in A_{\text{search}}$

6: **End For**

7: Search inside A_{search} for all orientation points in sight $\{n\}$ and sort them according to their distance to v_i .

8: **For** each $n_i \in \{n\}$ **Do**

9: **If** n_i inside valid area A_{search} **Then**

10: insert edge (v_i, n_i) to G

11: cut cone-shaped section $A_{\text{cone}_{v_i}}$ around edge (v_i, n_i) : $A_{\text{search}} = A_{\text{search}} \setminus A_{\text{cone}_{v_i}}$

12: **End If**

13: **End For**

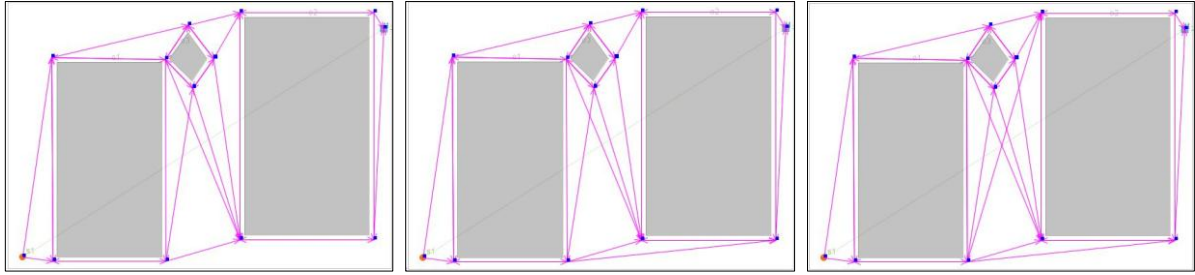
14: **End For**

268

269

Figure 7: Pseudo-code for graph generation algorithm

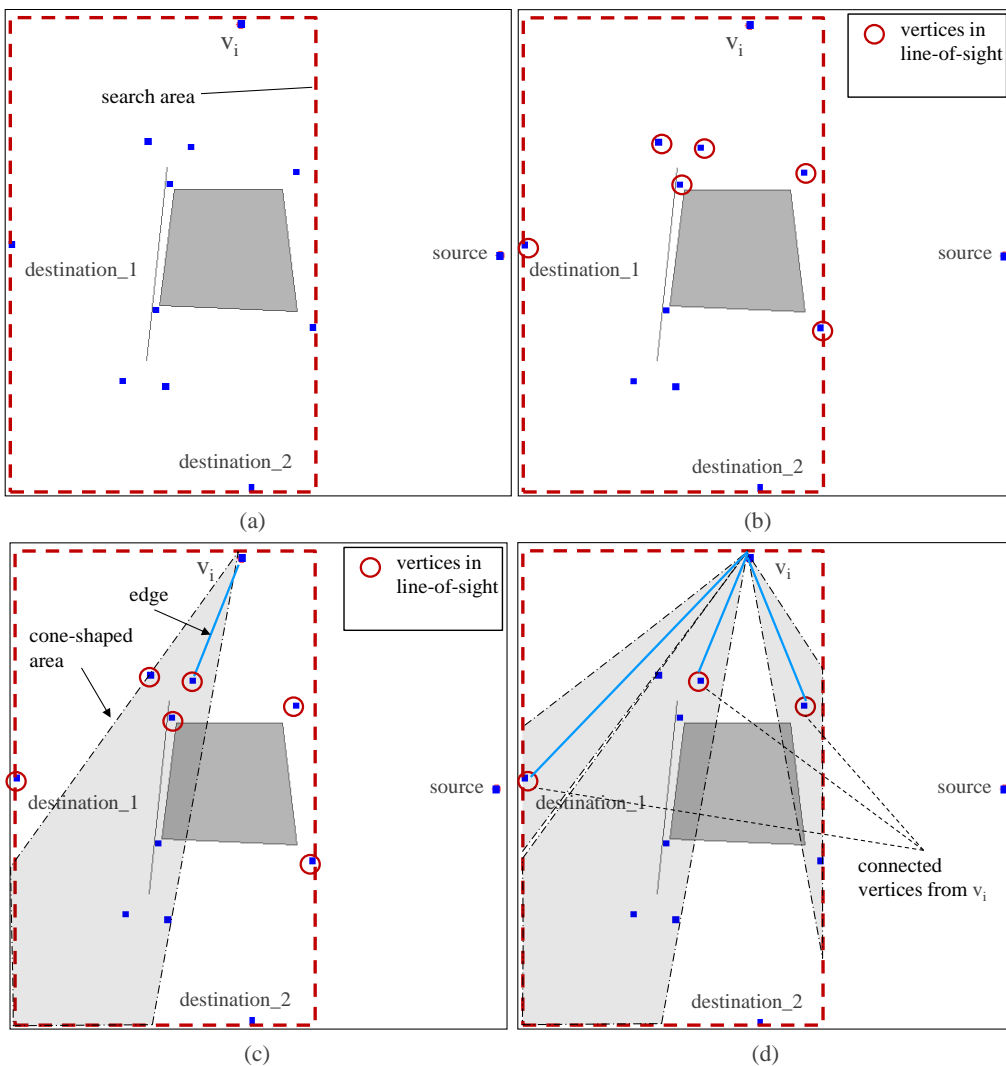
270 The number of the resulting edges can be varied by changing the value of the angle α_{cone} ,
 271 which defines the cone-shaped sections. Larger angles correspond to sparser graphs, since
 272 larger cones are removed from the search area. In Figure 8, different graphs for different
 273 values α_{cone} are illustrated. For all further examples, we chose an angle $\alpha_{\text{cone}} = \pi/20$.
 274



275

276 **Figure 8: Resulting graphs for different alpha values: Left: $\alpha_{\text{cone}} = \pi/15$; Middle: $\alpha_{\text{cone}} = \pi/20$; Right: $\alpha_{\text{cone}} =$**
 277 **$\pi/25$**

278 The resulting graph provides at least one route from each source to every destination if there
 279 is one. This follows directly from the algorithm: by definition, there is at least one navigation
 280 point in the line of sight in each search area. Thus each vertex is connected to at least one
 281 other vertex. This connected vertex refers either to the destination itself or it is connected to a
 282 vertex which leads around an obstacle that obstructs the sight line between this vertex and the
 283 destination. Accordingly, there is either a path from the start vertex to the destination or no
 284 connection at all between source and destination. Since the search is directed, the order of the
 285 inspected vertices can be chosen arbitrarily, but the resulting graph always remains the same.
 286



287

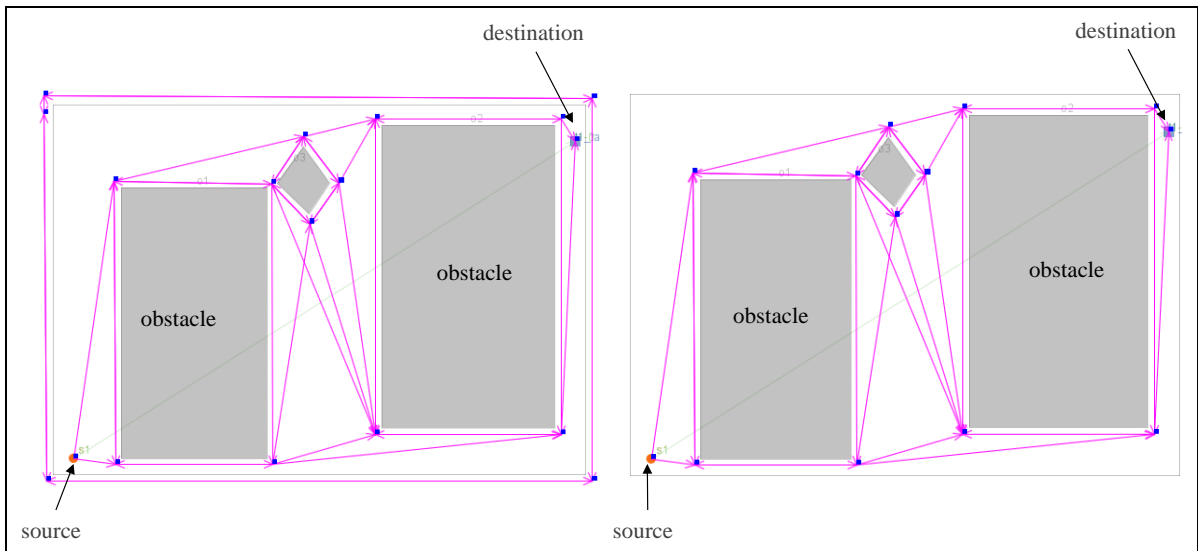
288 **Figure 9: Steps connecting node v_i with neighbours: (a) defined search area (b) all vertices visible from v_i**
 289 **(c) cone-shaped section for excluding vertices in same direction (d) resulting edges from vertex v_i**
 290

291 **4.3 Connectivity check**

292 An essential feature of the visibility graph is to provide at least one route leading from all
293 sources to all assigned destinations. A check is undertaken to ascertain if there are any
294 vertices that are not connected to any source or destination. This is likely because the
295 algorithm inspects every given navigation point (i.e. vertex). These vertices and their
296 corresponding edges can be discarded. To remove these, the connected components are first
297 identified within the graph [26]. This is done using a breadth-first iterator which starts from
298 each source vertex and checks if at least one destination can be reached. If so, the source and
299 destination belong to a connected component and all vertices of this connected component are
300 going to be kept.

301 Figure 10 shows an example of a graph consisting of two connected sets, but only one set
302 contains source and destination: the second set can, therefore, be discarded.

303 Note, that by applying this technique the resulting graph is no longer generic but directly
304 depends on the locations of sources and destinations within the scenario. This reduced graph
305 improves the performance of the route-finding algorithms.
306



307
308 **Figure 10: A graph with two connected sets (left) and a graph with only one connected set that contains**
309 **source and destination (right)**

310 **5 Application areas for the extended plain simulation with a navigation**
311 **graph**

312 Using this visibility graph as a navigation graph, more complex situations can be modelled as
313 well as different pedestrian behaviours with respect to large-scale orientation. The pedestrians
314 of the simulation are no longer shortsighted, but can react to situations which occur further
315 away (such as congestion). An example of using this graph to assist security staff can be
316 found in [27]. In the following, we introduce the mapping of different walking behaviours
317 using this graph.

318 5.1 Modelling different pedestrian behaviour

319 This graph can be used to model individual pedestrian behaviour. There are different
320 algorithms, which take into account the different behaviour of simulated pedestrians.

321 Pedestrians are categorised into three different main types:

- 322 • Pedestrians who are very familiar with the environment and will choose an alternative
323 route if their current route is very crowded.
- 324 • Pedestrians with no detailed local knowledge who only know the direction of the
325 destination but no details about the specific route.
- 326 • Pedestrians who are not familiar with the location and make their decisions based on
327 local criteria: The choice of the next turn depends on the characteristics of the
328 outgoing edges (long edges vs. short edges) and the route choices of other pedestrians.

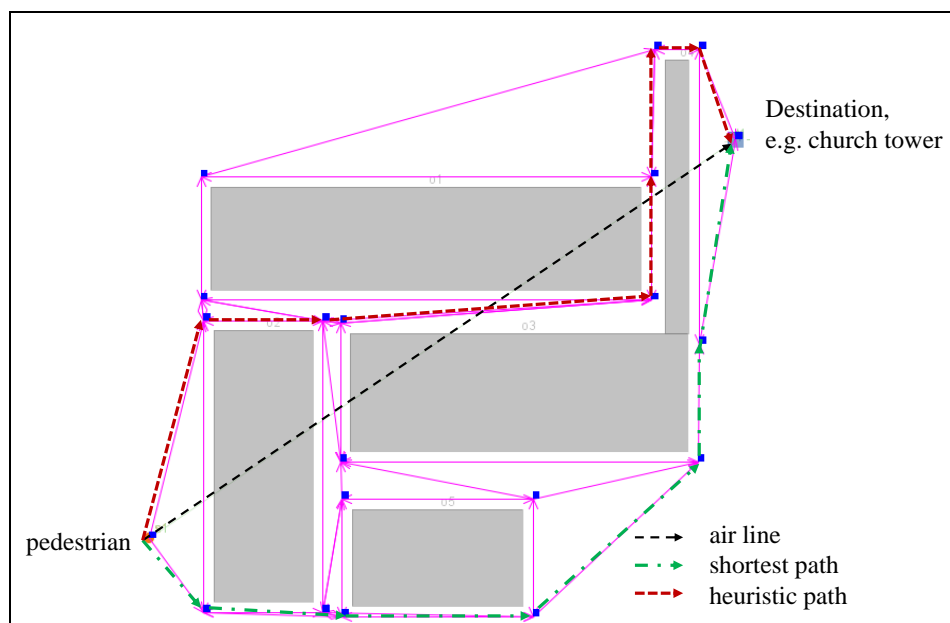
329

330 Pedestrians with detailed local knowledge are modelled using the *Fastest Path Algorithm*.
331 The fastest path is calculated using the Dijkstra Shortest Path Algorithm [28] with dynamic
332 edge weights, taking travelling times instead of distances as edge weights. Hence the assigned
333 edge weights can change over time. We derive this travel time from the density on an edge
334 and the corresponding mean velocity. A detailed description of the algorithm can be found in
335 [23].

336

337 Pedestrians, who employ an air-line (as the crow flies) distance between their current location
338 and the destination for navigating through a scenario they are not familiar with, are modelled
339 by applying a variant of the *A* Algorithm* [29]. The basic idea of this heuristic algorithm is to
340 take given information into account and combine it with assumptions about missing
341 information. In our case, the given knowledge is the direction to the destination (the exact
342 route is outside the field of vision) and the current distance to the next navigation point, i.e.
343 vertex (the visibility graph ensures that the information is always available).

344



345

346 **Figure 11 Example for the heuristic A* algorithm: due to the air-line estimation, the algorithm does not**
347 **find the shortest path, but the path that most approximates the air-line to the destination**

348 To implement this, the algorithm uses real distance edge weights (or as an alternative travel
349 times) for the known part of the route and an additional heuristic measure for the unknown
350 part. This unknown part refers to the air-line distance to the destination to estimate the
351 unknown part. Figure 11 shows an example that illustrates the basic idea of the algorithm.

352 The navigation behaviour of the third type of pedestrians is modelled by a *Probabilistic*
353 *Choice Algorithm*. With this algorithm, local-based decisions as well as non-deterministic
354 route-choice behaviour of pedestrians are modelled. Furthermore, it reflects the “trail
355 behaviour” of pedestrian, i.e. the tendency to follow paths chosen by other pedestrians. The
356 algorithm is implemented according to [30]:

357 Different values of an edge, such as its derivation from the air-line to the destination as well
358 as the length of the edge and improvement of distance to destination, are totalled. This
359 combined value is its edge weight. At each node, the weight of each outgoing edge is scaled
360 to a value between 0 and 1, such that the sum of all edge weights is 1. Using roulette wheel
361 selection [31], one of the possible outgoing edges is chosen: The higher the value of an edge,
362 the higher the probability that it is selected.

363 To map the “trail behaviour”, each chosen edge is assigned an amount of pheromone, which
364 evaporates over time according to Ant Colonization Optimization algorithms [32].

365 A detailed definition including validation of individual behaviour as well as the description of
366 the algorithms can be found in [33].

367 This algorithm differs from the Route Choice Self Organization (RSCO) algorithm proposed
368 in [14] in such way, that Teknomo defines three different principles for edge selection: the
369 permission (whether an edge is accessible), the interaction (avoidance of crowded edges) and
370 navigation (relative enhancement to the destination). The *Probabilistic Choice Algorithm*
371 does not take into account any densities on the edges as a parameter for avoiding congested
372 edges, but instead it models the trail behaviour by means of evaporating pheromone, meaning
373 that pedestrians, who are unfamiliar with the location, will choose an edge more likely, if
374 there are already pedestrians walking along this edge. Secondly and more importantly, in
375 contrast to the RSCO algorithm the *Probabilistic Choice Algorithm* is not deterministic with
376 respect to edge choice.

377 **5.2 Test case**

378
379 The developed graph generation method and navigation strategies have been applied on an
380 example scenario shown in Figure 10 (right). Here, pedestrians walk from the lower left
381 corner to the upper right corner within a room. Three obstacles are located inside this room. In
382 total, 1200 pedestrians were simulated with a generation rate of 6 pedestrians per second.

383 In a first simulation the graph layer was not used. Simulation runs using the navigation graph
384 were then conducted: pedestrians walked according to the three algorithms *Fastest Path*, *A**
385 and *Probabilistic Choice*. The last simulation was based on a combination of all three
386 algorithms.

387 Figure 12 to Figure 16 show screenshots of the simulations at different points in time:
388 Without using a graph, each simulated pedestrian takes the same route. As shown in Figure
389 12, this results in significant congestion in front of the bottleneck of the right obstacle. This is
390 because simulations without a navigation graph update a pedestrian’s position solely using the
391 cellular automaton. During the simulation, all neighbouring cells are examined for each
392 pedestrian at each time step, choosing the cell with the lowest potential value if it is not

393 occupied by either an obstacle or another pedestrian. This selection process is conducted until
394 all pedestrians reach their destination. From this setup it is obvious that each pedestrian is
395 short sighted and chooses a similar route to walk to his destination. The only varying factor is
396 the number of pedestrians that walk the same way and occupy cells.

397 Figure 13 shows the pedestrians walking according to the *Fastest Path Algorithm*. One can
398 see a wider spread of routes resulting from the dynamic routing. To begin with, the fastest
399 path is identical to the shortest path. After a while, the route becomes too crowded. The route
400 south of the first obstacle becomes faster, since pedestrians taking the shortest route have to
401 slow down in response to the intensity of its use. Later in the simulation, a third route
402 becomes the fastest, as the last part of the two former routes are crowded on the last common
403 segment.

404 In Figure 14, the results of the *A* Algorithm* are illustrated. In spite of the results of the
405 *Fastest Path Algorithm*, the most likely way to the destination is south of the left obstacle.
406 This is explained by the fact that the lower route is located closer to the air-line to the
407 destination. However, as with the *Fastest Path Algorithm*, the route becomes too crowded
408 after a while and pedestrians start to walk on the west side of the left obstacle. This happens,
409 since travel times are used as fixed edge weights instead of Euclidean distances. At some
410 point, the bottleneck north of the right obstacle becomes crowded and pedestrians start to
411 walk along the south of the right obstacle.

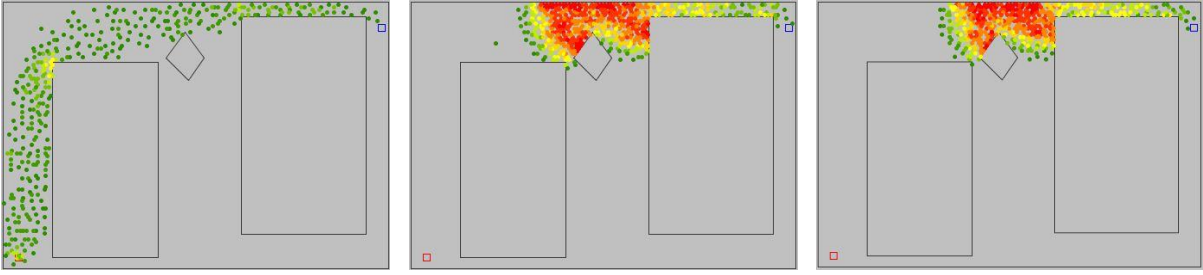
412 The results of the *Probabilistic Choice Algorithm* are demonstrated in Figure 15. Initially,
413 there is a wide spread of the pedestrians' route choices, since edges are chosen by probability.
414 After a while, the path north of both obstacles becomes more likely, due to greater pheromone
415 deposition. Not taking into account the densities on the edges, the pattern seen in the plain
416 simulation happens, namely congestion in front of the upper left corner of the right obstacle.
417 This reflects exactly what was supposed to be modelled: if a person is not familiar with a
418 place, he will most likely stay on his path, since he does not know alternative routes that lead
419 to the destination.

420 Each algorithm on its own maps only one kind of pedestrian behaviour. Combining all
421 algorithms, the simulation produces the results shown in Figure 16. The number of
422 pedestrians for each type is chosen according to a distribution rate, which has been derived by
423 the experiment presented in [33], in which large scale orientation is investigated: Students are
424 sent to a well-known location in the Munich city centre (Germany) without a map. On their
425 return, they document the path they have chosen. Additionally, each participant fills out a
426 questionnaire regarding way-finding behaviour and orientation. From the analysis of the
427 documented paths and the questionnaire, a distribution rate for the different types of
428 orientation has been derived.

429 One can observe that no high densities occur at any location. Likewise, the different
430 navigation behaviours seem to be reflected well, since one can identify the preferred routes of
431 each algorithm.

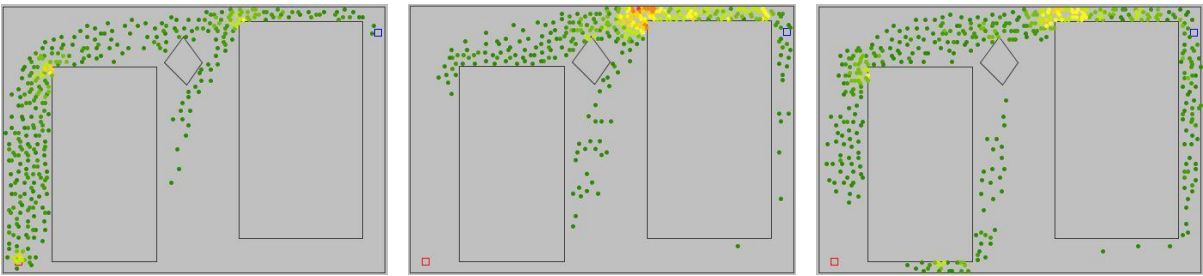
432 Nevertheless, the results of the experimental simulation need to be validated to ascertain how
433 realistic they are. We can, however, clearly see that the simulation becomes more realistic
434 when we apply a navigation graph, since unlikely congestions no longer occur. Realistic in
435 this context means that assuming a certain distribution rate of the simulated pedestrians' local
436 knowledge as given, the simulation is able to reflect these different route choice behaviours
437 accordingly.

438



439 **Figure 12: Screenshot of a simulation of 1200 pedestrians walking from the lower left corner**
 440 **to the upper right corner *without using a navigation graph***
 441 **after 63 seconds (left), 263 seconds (middle) and 284 seconds (right).**

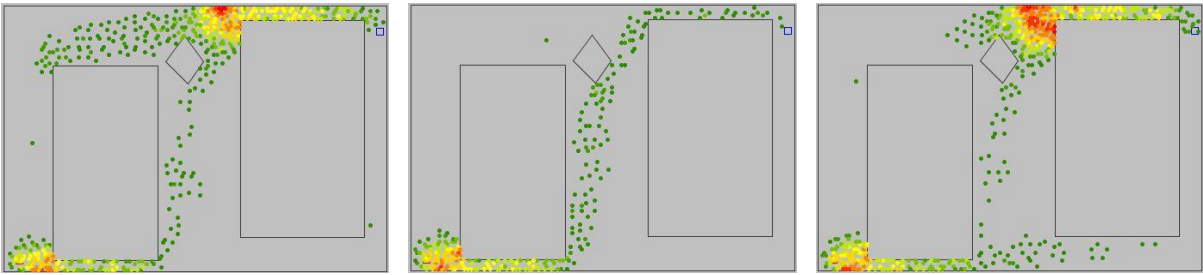
442



443

444 **Figure 13: Screenshot of the same simulation using a navigation graph with *Fastest Path Algorithm***
 445 **after 63 seconds (left), 263 seconds (middle) and 284 seconds (right)**

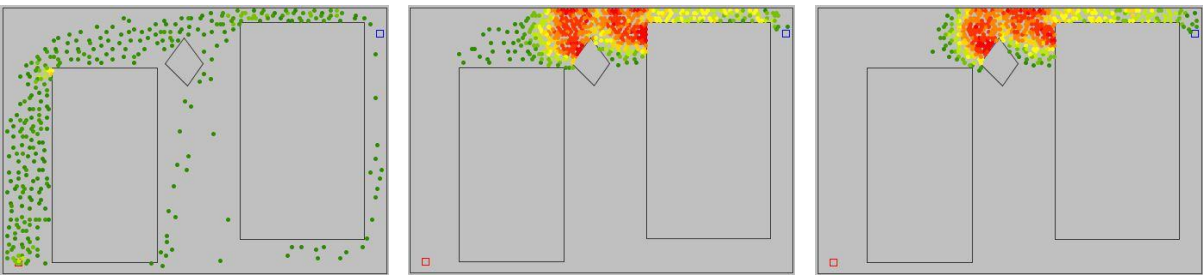
446



447

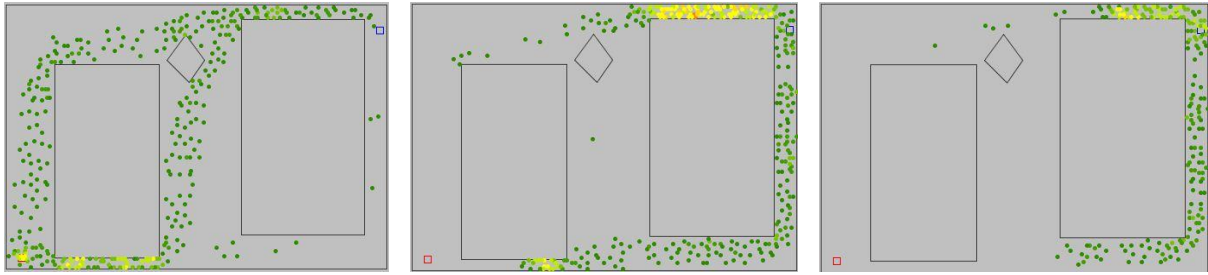
448 **Figure 14: Screenshot of the same simulation using a navigation graph with *A* algorithm***
 449 **after 63 seconds (left), 263 seconds (middle) and 284 seconds (right)**

450



451

452 **Figure 15 Screenshot of the same simulation using a navigation graph with *Probabilistic Choice* after 63**
 453 **seconds (left), 263 seconds (middle) and 284 seconds (right)**



454

455

456

Figure 16 Screenshot of the same simulation using a combination of the above algorithms after 63 seconds (left), 263 seconds (middle) and 284 seconds (right)

457

5.3 Real-world application scenario

458

459

460

461

462

463

464

To illustrate the application of the developed simulation approach, we are discussing a real-world application scenario. Here, an architect or engineer responsible for the layout of an office building is using the graph-extended pedestrian simulation to investigate different options with respect to the number and localisation of (emergency) exits. The office building has 4 floors. The investigated floor plan comprises 41 offices (Figure 17). For each office, the number of expected occupants is known. In the first layout option, there is one exit stair located on the west side and another one located on the east side (see Figure 17).



465

466

Figure 17 Floor plan of the investigated office building with 41 offices

467

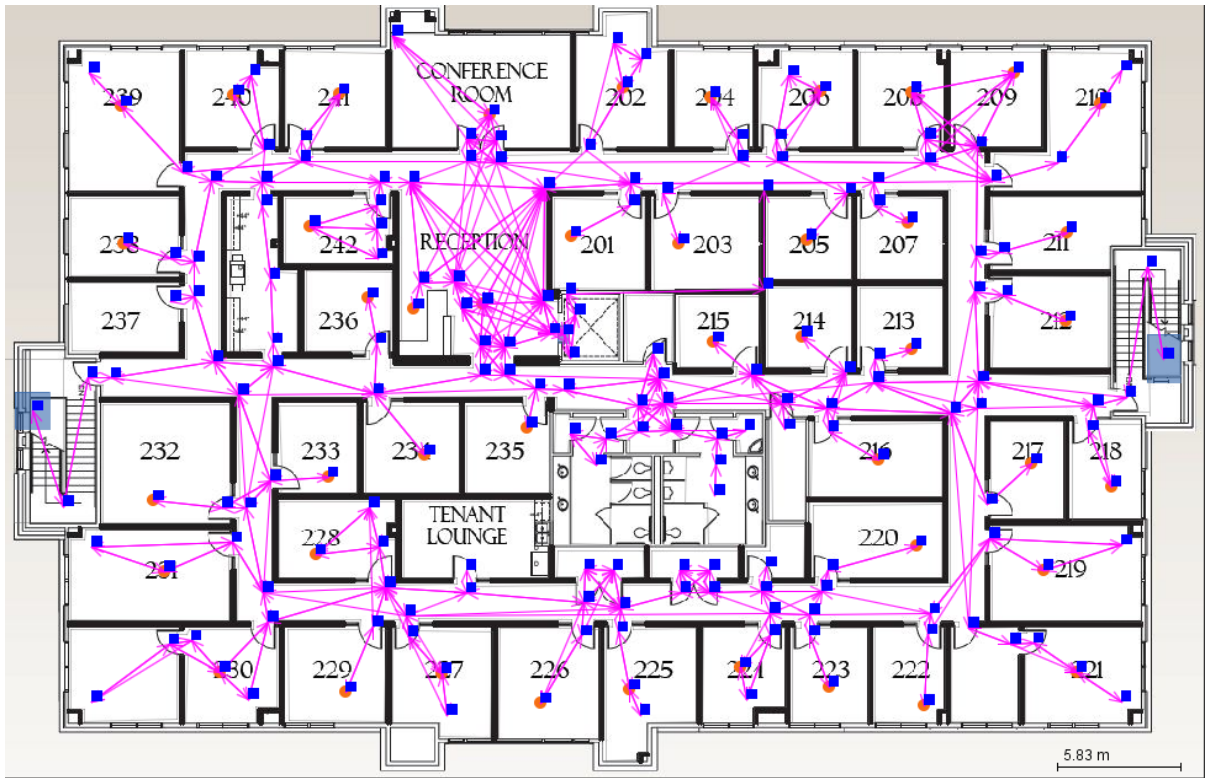
468

469

470

By means of the methodology introduced in Section 4, a navigation graph is automatically generated for the given floor plan. The result is depicted in Figure 18. The scenario has been simulated for a total number of 161 pedestrians. At the start of the simulation they are placed according to the given number of occupants for each individual room. Each exit stair has been

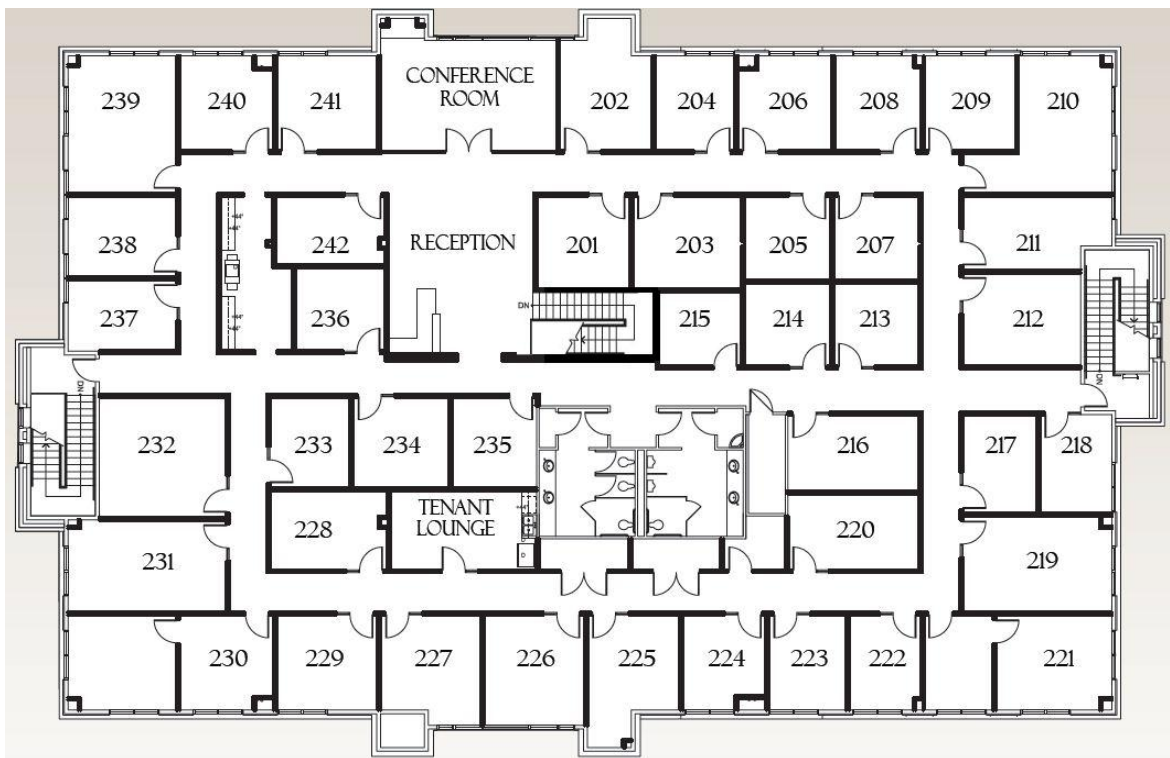
471 assigned a suitable capacity. Each pedestrian is routed towards the exit which is closest to
472 his/her original position.



473

474

Figure 18 The automatically generated navigation graph.



475

476

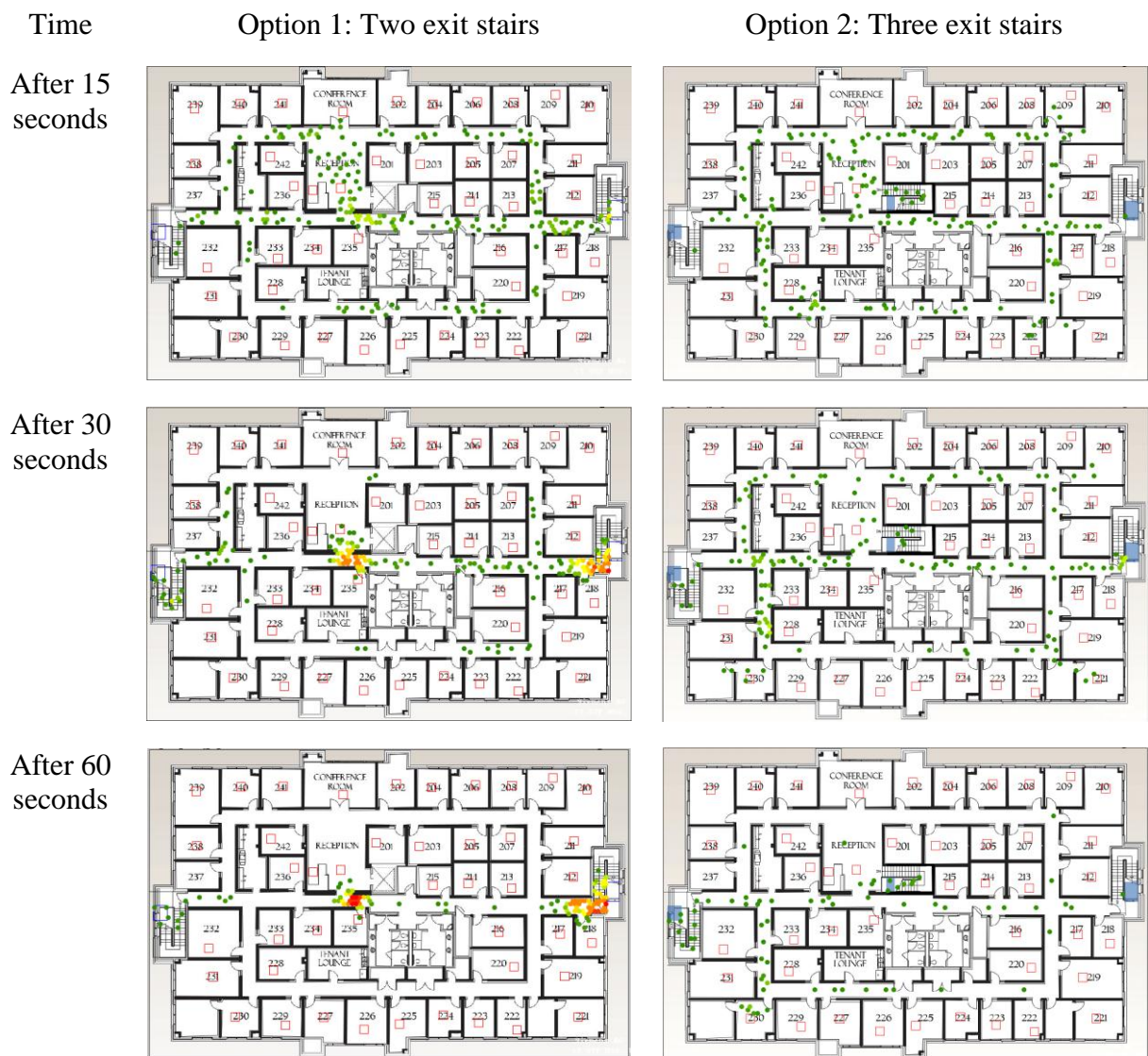
Figure 19 Modified floor plan: An additional stair has been placed at the central position.

477 The simulation results, depicted in Table 1 left-hand side, show that this setup results in
 478 congestion in front of the stair. In an emergency situation, such constellations must be
 479 avoided.

480 For this reason, in the second option an additional stair has been placed in the floor at a
 481 central position (Figure 19). Again, the navigation graph is automatically generated. The
 482 results of the subsequent simulation run are depicted in Table 1, right hand side. It can be seen
 483 that in this option, no congestions occur and thus a critical situation is avoided.

484 The engineer can take these simulation results into account for the final decision regarding the
 485 number and position of the exit stairs. The automated navigation graph generation method
 486 introduced in this paper provides the possibility for a quick and effortless evaluation of floor
 487 plan alternatives with respect to evacuation situations.

488



489 **Table 1 Results of the simulation: The left column depicts the simulation results for the two exit stairs**
 490 **option, the right columns shows the results for the three exit stairs option. Whereas for the first option**
 491 **critical congestion occur during an evacuation, they do not so for the second option.**

492 **6 Discussion**

493 Engineers responsible for the layout of public buildings and large event areas have to consider
494 the movement and behaviour of pedestrian crowds in order to prevent critical situations.
495 Recently, computational simulations have been increasingly used to predict the dynamics of
496 pedestrian crowds. However, most of the available simulation systems either rely on rather
497 simple pedestrian navigation models, which reflect human behaviour only in a very limited
498 manner, or are computationally very expensive. In this paper, a sophisticated graph-based
499 approach has been presented, which allows integrating advanced navigational behaviour with
500 computationally efficient simulations.

501 The implementation of this approach includes an advanced technique for generating sparse
502 navigation graphs from a given spatial layout of the scenario under investigation. This graph
503 is a subset of a standard visibility graph. It can be used to not only map individual pedestrian
504 behaviour in pedestrian simulations, but also to model the large-scale orientation of
505 pedestrians.

506 The advantage of using such a navigation graph instead of using an agent-based approach is
507 an enormous reduction in computational effort. Furthermore, a scenario can be easily changed
508 during runtime. Closing doors or making routes non-accessible, for example due to fire, can
509 be modelled simply by deleting the corresponding edges.

510 The paper introduces a new method for constructing a navigation graph from a given
511 geometry by reducing a visibility graph with a cone-based search method. The main
512 advantage of the method is that the resulting graph is very sparse. Unlike standard visibility
513 graphs, geometrically close edges are merged into a single edge, while at the same time
514 maintaining broad spatial coverage for ensuring a better modelling of navigational behaviour.
515 Furthermore, all vertices are discarded that are not part of any connected component with
516 sources as well as destinations.

517 To measure the quality of the resulting graph, a next step in our research will be to define a
518 metric and evaluate the navigation graph according to this metric in comparison to existing
519 graphs.

520 To demonstrate the advantage of a graph-extended simulation, the results of a set of sample
521 simulation scenarios have been presented. Different levels of local knowledge are modelled
522 using three different routing algorithms: Pedestrians who are familiar with a location are
523 simulated using a *Fastest Path Algorithm*. Pedestrians with partial knowledge of a location
524 are modelled according to the heuristic *A* Algorithm*. The movements of pedestrians with no
525 local knowledge are modelled using the *Probabilistic Choice Algorithm* – a derivation of an
526 Ant Colonization Algorithm. The application of these three algorithms within the simulation
527 improved the simulation results significantly, since artificial congestions produced by the
528 static cellular automaton model could be eliminated. Furthermore, a wide range of diverging
529 route choice behaviour is realized, i.e. not just the shortest routes are taken by the simulated
530 persons, but also non-optimal ones, which reflects human navigation more naturally. In
531 addition to the modelling of different route choices, the application of the navigation graph
532 resolves the problem of short-sightedness in conventional simulation models and makes it
533 possible to consider the pedestrians' sense of large-scale orientation.

534 In future research we plan to continue validating the simulation results to ensure the quality of
535 the different routing algorithms. According to these validation results, we will further improve
536 the algorithm and incorporate interactions between the different types of pedestrians.

537

538

539

540 **References**

- 541
- 542 [1] A. Schadschneider, W. Klingsch, H. Klüpfel, T. Kretz, C. Rogsch, A. Seyfried, Evacuation
543 dynamics: Empirical results, modeling and applications, *Encyclopedia of Complexity and System*
544 *Science* (2009) 3142–3176.
- 545 [2] H.W. Hamacher, S.A. Tjandra, Mathematical modelling of evacuation problems: A state of the
546 art, in: M. Schreckenberg (Ed.), *Pedestrian and Evacuation Dynamics*, Springer, Berlin, 2002, pp.
547 227–266.
- 548 [3] D. Helbing, A fluid-dynamic model for the movement of pedestrians, in: *Complex Systems*,
549 1992, pp. 391–415.
- 550 [4] L.F. Henderson, The Statistics of Crowd Fluids, *Nature* 229 (1971) 381–383.
- 551 [5] D. Helbing, P. Molnár, Social Force Model for Pedestrian Dynamics, *Physical Review E* 5 (1995)
552 4282–4286.
- 553 [6] C. Burstedde, K. Klauck, A. Schadschneider, J. Zittartz, Simulation of pedestrian dynamics using
554 a two-dimensional cellular automaton, *Physica A: Statistical Mechanics and its Applications* 3-4
555 (2001) 507-525.
- 556 [7] N. Ronald, L. Sterling, M. Kirley, An Agent-Based Approach To Modelling Pedestrian
557 Behaviour, *Lecture Notes in Computer Science* (2007) 145-156.
- 558 [8] N. Pelechano, A. Malkawi, Evacuation simulation models: Challenges in modeling high rise
559 building evacuation with cellular automata approaches, *Automation in Construction* 4 (2008)
560 377–385.
- 561 [9] C. Reynolds, Steering Behaviors for Autonomous Characters, in: *Game Developers Conference*,
562 1999.
- 563 [10] S.R. Musse, D. Thalmann, A Model of Human Crowd Behavior: Group Inter-Relationship and
564 Collision Detection Analysis, in: *Workshop Computer Animation and Simulation of*
565 *Eurographics*, 1997, pp. 39-52.
- 566 [11] F. Durupinar, J.M. Allbeck, N. Pelechano, N. Badler, Creating crowd variation with the OCEAN
567 personality model, in: *Proceedings of the 7th international joint conference on Autonomous*
568 *agents and multiagent systems - Volume 3, International Foundation for Autonomous Agents and*
569 *Multiagent Systems*, Richland, SC, 2008, pp. 1217-1220.
- 570 [12] A. Lerner, Y. Chrysanthou, D. Lischinski, Crowds by Examples, in: D. Cohen-Or, P. Slavík
571 (Eds.), *EUROGRAPHICS 2007*, 2007.
- 572 [13] M. Asano, T. Iryo, M. Kuwahara, Microscopic pedestrian simulation model combined with a
573 tactical model for route choice behaviour, *Transportation Research Part C: Emerging*
574 *Technologies* 6 (2010) 842–855.
- 575 [14] K. Teknomo, Modeling mobile traffic agents on network simulation, in: *Proceeing of the 16th*
576 *Annual Conference of Transportation Science Society of the Philippines (TSSP)*, Manila, 2008.
- 577 [15] H.M. Choset, *Principles of robot motion*, MIT Press, Cambridge, Mass., 2005.
- 578 [16] S.M. LaValle, *Planning Algorithms*, Cambridge University Press, Cambridge, U.K, 2006.
- 579 [17] F. Aurenhammer, Voronoi Diagrams - A Survey of a Fundamental Geometric Data Structure,
580 *ACM Comput. Surv.* (1991) 345-405.
- 581 [18] A. Sud, E. Andersen, S. Curtis, M.C. Lin, D. Manocha, Real-Time Path Planning in Dynamic
582 Virtual Environments Using Multiagent Navigation Graphs, *IEEE Transactions on Visualization*
583 *and Computer Graphics* (2008) 526-538.
- 584 [19] O. Arikan, S. Chenney, D.A. Forsyth, Efficient multi-agent path planning, in: *In Proceedings of*
585 *the 2001 Eurographics Workshop on Animation and Simulation*, 2001, pp. 151-162.
- 586 [20] C. Gloor, P. Stucki, K. Nagel, Hybrid Techniques for Pedestrian Simulations, in: P. Sloot, B.
587 Chopard, A. Hoekstra (Eds.), *Cellular Automata*, Springer Berlin / Heidelberg, 2004, pp. 581–
588 590.
- 589 [21] W. Klein, G. Köster, A. Meister, Towards The Calibration of Pedestrian Stream Models, in: J.
590 Weglarz, R. Wyrzykowski, B. Szymanski (Eds.), *8th Int. Conf.on Parallel Processing and*
591 *Applied Mathematics*, Springer, Berlin, 2010.
- 592 [22] D. Hartmann, Adaptive pedestrian dynamics based on geodesics, *New Journal of Physics* 4
593 (2010) 43032.

- 594 [23] M. Höcker, V. Berkhahn, A. Kneidl, A. Borrmann, W. Klein, Graph-based approaches for
595 simulating pedestrian dynamics in building models, in: University College Cork (Ed.), 8th
596 European Conference on Product & Process Modelling (ECPPM), Cork, Ireland, 2010.
- 597 [24] A. Kneidl, A. Borrmann, D. Hartmann, Einsatz von graphbasierten Ansätzen in einer
598 mikroskopischen Personenstromsimulation für die Wegewahl der Fußgänger, in: T. Krämer, S.
599 Richter, F. Enge, B. Kraft (Eds.), Forum Bauinformatik 2010, Shaker, Aachen, 2010.
- 600 [25] N. Beckmann, H.-P. Kriegel, R. Schneider, B. Seeger, The R*-tree: an efficient and robust access
601 method for points and rectangles, SIGMOD Rec. 2 (1990) 322-331.
- 602 [26] A. Gibbons, Algorithmic graph theory, Cambridge Univ. Press, Cambridge, 1999.
- 603 [27] A. Kneidl, M. Thiemann, D. Hartmann, A. Borrmann, Combining pedestrian simulation with a
604 network flow optimization to support security staff in handling an evacuation of a soccer stadium,
605 in: Proceedings of European Conference Forum 2011, Cork, Cork, 2011.
- 606 [28] E.W. Dijkstra, A note on two problems in connexion with graphs, Numer. Math. 1 (1959) 269.
- 607 [29] Y. Li, M. Höcker, Heuristische Navigationsalgorithmen für Fußgängersimulationen, in: P. von
608 Both (Ed.), Forum Bauinformatik 2009, Universitätsverl., Karlsruhe, 2009, pp. 25–36.
- 609 [30] D. Angus, Solving a unique Shortest Path problem using Ant Colony Optimisation.
- 610 [31] T. Bäck, Evolutionary algorithms in theory and practice, Oxford Univ. Press, New York, 1996.
- 611 [32] M. Dorigo, Optimization learning and natural algorithms, Dissertation, Mailand, 1992.
- 612 [33] A. Kneidl, A. Borrmann, How Do Pedestrians find their Way? Results of an experimental study
613 with students compared to simulation results, in: W. Jaskolowski, P. Kepka (Eds.), EMEVAC,
614 The Main School of Fire Service, Warsaw, 2011.
- 615